Time-resolved x-ray monitoring of laser ablation of and plasma formation from Si

H. van Brug, K. Murakami,[a] F. Bijkerk, and M. J. van der Wiel
FOM Institute for Atomic and Molecular Physics, Kruislaan 407, 1098 SJ Amsterdam, The Netherlands

(Received 3 June 1986; accepted for publication 22 July 1986)

We present x-ray absorption measurements on silicon clusters and silicon plasmas produced by pulsed laser irradiation of bulk silicon. The results are compared with earlier time-resolved x-ray absorption measurements on amorphous silicon foils under pulsed laser irradiation. Clusters are formed at an irradiance as low as 3.0 J/cm^2. At an irradiance of 14 J/cm^2 ionized species up to Si^{4+} are formed. We find a removed Si layer thickness of 80 Å at an irradiance of $\approx$6 J/cm^2, at 15 ns pulse duration.

I. INTRODUCTION

In the past several years, considerable work has been done to understand the phenomena occurring in the bulk during pulsed laser annealing of amorphous silicon.[1–3] Other groups have investigated the desorption process of silicon clusters under pulsed laser irradiation.[4–7] These two fields were always discussed separately. In this paper we discuss both fields, in order to combine these two subjects.

Previously,[8] we performed x-ray L-absorption measurements in the 100–300 eV range on amorphous Si foils with carbon backing for strength (600 Å Si on 400 Å C). We measured the laser energy dependence and time dependence of the annealing process and determined the energy density range within which annealing takes place. Here are the summarized results. In range I, from 0 up to $\approx$0.17 J/cm^2, the foil is only heated, not annealed. In range II, from $\approx$0.17 to 1 J/cm^2, annealing takes place. Range III, above 1 J/cm^2, is the damaging range. In range III, sharp line structures appear in the absorption spectra above the $L_{II,III}$ edge, between 110 and 150 eV, and the $L_{II,III}$ edge shifts to higher energies, compared to the edge position for the un-irradiated foil ($\approx$110 eV, instead of $\approx$100 eV). The structures could be assigned partly as absorption lines of Si^{4+} ions. It was concluded that in range III the foil is damaged, and that particles are emitted. The particles emitted from the surface are Si atoms, small sized clusters and/or Si ions, depending on the energy density used. We found from the spectra recorded at 60 ns after the laser anneal pulse that the line structure decreases drastically and that the spectrum resembles the one for the annealing case, range II, very closely.

It is known in literature that during laser irradiation Si clusters can be formed. In Refs. 7 and 9 the creation of small sized clusters is described. The size of these clusters is approximately 5 to 10 atoms per cluster. In Ref. 10 it is discussed that large sized "liquid" clusters are emitted from the surface. This is explained by the following model. The clusters are ejected from the surface due to superheating of the subsurface region during the laser irradiation, before the surface itself has reached the vaporization temperature. This thermal strain may blow the liquid layer away from the surface in the form of liquid clusters.

In order to get more information on these processes in range III, we measured the absorption spectra for Si particle clouds, created by pulsed laser irradiation of bulk Si. From these measurements we derived a model explaining the time behavior in the first 60 ns of the formation of clusters, and we show the resemblance between these spectra and those of molten Si foils.

These are the first x-ray absorption recordings of Si clusters, neutral atoms, and ions. The ion and neutral production by pulsed laser irradiation of Si is often reported but the process is never described for short time scales. The only description is given for a timescale of milliseconds.

II. EXPERIMENT

For an outline of the apparatus see Fig. 1. As x-ray source we used a laser-produced plasma (LPP). The laser is a pulsed, frequency doubled neodymium:yttrium aluminum garnet/glass system, producing pulses of 8 J of 532 nm light in 15 ns. The output beam is focused down to a spot with a diameter of 65 μm on a metal cylinder (for the measurements presented here we used a Ta laser target). The power density in this focus is 1×10^{13} W/cm^2. The plasma thus created gives an x-ray yield of approximately 10^{10} photons per pulse in the energy range 90–190 eV. An image of the plasma is created outside the source chamber by means of a collecting toroidal mirror, with an amplification of a factor 2. In this intermediate focus the absorption measurements were performed. The advantage of measuring in a focus is that homogeneity of the sample is required only over a small area. Because the x-ray beam is undispersed, the homogeneity is not even very important. The transmitted beam is dispersed by a grating and the full spectrum recorded on a gold photoelectrode. Registration of the photoelectron yield across the full electrode on a position-sensitive detector, provides the possibility of single shot spectral measurements, with 15 ns time resolution. The electron yield is recorded by a multichannelplate/phosphor-screen assembly and an optical multichannel detector. The positional information is conserved by a 0.12-T magnetic field. The energy resolution of our apparatus is $\approx$4 eV. For a more detailed description of the apparatus see Refs. 11–13.

In order to measure x-ray absorption spectra of laser irradiated samples, we split the laser beam into a pump and a

[a] Permanent address: Institute of Materials Science, University of Tsukuba, Sakura, Ibaraki 305, Japan.

 0021-8979/86/223438-06$02.40

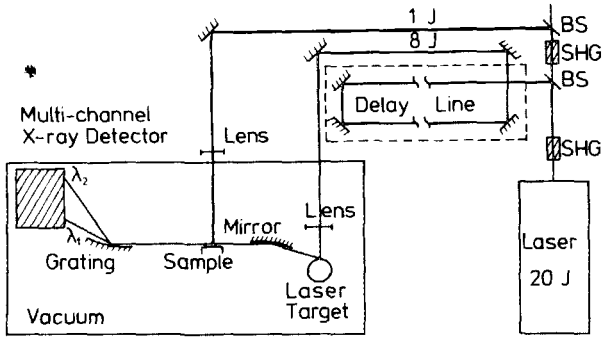

FIG. 1. Experimental setup for time-resolved x-ray absorption. A 20-J Nd:YAG/glass system laser pulse (15 ns) is frequency doubled (SHG) twice to give a 1-J pump beam and a 8-J probe beam. The latter can be delayed by up to 60 ns (BS—beamsplitter). The 8 J probe beam creates a plasma which emits a continuum of soft x rays. After transmission through the sample (either a foil or a cloud of particles), the x rays are dispersed by a polychromator and detected by a multichannel x-ray detector. Complete x-ray absorption spectra from 90 to 190 eV are recorded in one laser shot.

probe part. The pump part is used to irradiate the sample (≈ 1 J), and the probe part (≈ 8 J) to create the x-ray producing plasma with a variable time delay with respect to the pump pulse. The delay time can be varied by changing the light path length of the probe pulse. Delay times used are 12, 30, and 60 ns (see Fig. 1). In order to measure an absorption spectrum, we first measure with the sample in the intermediate focus, and obtain a spectrum $I(E)$, and then without the sample, which yields spectrum $I_0(E)$. I_0 is then divided by I to obtain the absorption signal of the sample, with removal of all the source characteristics and structures due to the optics. The sample was a piece of Si wafer of $20\times 6\times 2$ mm. The 2 mm side was in the direction parallel to the x-ray probe beam. The 6×2 mm face of the sample was irradiated with the laser pump beam, to produce a cloud of emitted particles, while the x-ray probe beam passed above this face at variable height. The 20 mm side was chosen parallel to the irradiating beam to make sure that particles emitted from the manipulator on which the sample is mounted, cannot be probed by the x rays. Of this cloud of particles, over the range from 0 to 1000 μm above the surface, we measured the absorption spectra. The zero point is taken as the position where half of the x-ray signal is blocked by the silicon. The probe beam diameter being 160 μm, the height above the surface must be larger than 80 μm to measure with a totally unblocked beam. The absorption measurements on the cloud of particles were performed at a delay time of 12 ns at energy densities of 3.5, 6.0, and 14.0 J/cm^2, and at a delay time of 60 ns at an energy density of 6.0 and 14.0 J/cm^2. The three energy densities were chosen such as to correspond to the value where emission just starts respectively where sufficient energy is available to form an ionized plasma, and to include one intermediate energy density.

III. RESULTS

The onset for detectable particle emission (onset for damage of the surface) was found in Ref. 4 to be at approximately 2.0 J/cm^2 for a 20-ps irradiating laser pulse. However, our measurements performed at the energy densities of 2.3 and 2.5 J/cm^2 show no detectable emission of particles at 15 ns laser pulses. The first observed x-ray absorption was at an irradiation energy density of 3.5 J/cm^2. In Figs. 2–4 the results of the x-ray absorption measurements are shown.

Figure 2(a) shows the x-ray absorption spectra in the 90–190 eV range, at a delay time of 12 ns and an energy density of 3.5 J/cm^2. For comparison a spectrum from the earlier foil measurements[8] is presented in Fig. 2(b). This spectrum was recorded with a delay time of 12 ns and an energy density of 0.7 J/cm^2 (anneal range). The different spectra in Fig. 2(a) are recorded at different heights of the center of the x-ray probe beam above the surface. Figure 3 shows the results for an energy density of 14 J/cm^2 at a delay time of 12 ns [Fig. 3(a)] and 60 ns [Fig. 3(b)]. In Fig. 3(c) a spectrum of the foil measurements is presented. This spectrum was recorded at a delay time of 12 ns and an energy density of 3.6 J/cm^2 (damage range). In Figs. 4(a) and 4(b) we show the results for the measurements at an energy density of 6.0 J/cm^2 and a delay time of 12 ns in part (a) and 60 ns in part (b). Figure 4(c) shows the same spectrum as Fig. 3(c). In Table I all spectral features and their symbols are summarized. These absorption features are labeled in the figures at the positions where their appearance is most pronounced. The physical origin of these features as given in Table I will be discussed in the following section. For a summary of all the absorption features in Figs. 2–4, see Table II.

IV. DISCUSSION

Absorption features expected to be seen in our energy range are the following: the L edges of liquid Si, of Si clusters, and of Si^0 to Si^{4+} atoms and ions. The energy positions of the $L_{II,III}$ and L_I edges of neutral Si and Si ions are not known experimentally, but they can be calculated from Hartree–Fock potentials, as has been done in Ref. 14, or from Slater–Zener orbitals. Both values are given in Table III. In addition, we expect features due to series of Rydberg absorption lines of atoms and ions in various states of ionization. In our energy window, from 90 to 190 eV, only the transitions from a core configuration $2s^2\,2p^6$, having 0 to 4 additional outer electrons, to $2s^2\,2p^5\,nl$ or $2s^1\,2p^6\,nl$ from $n=3$ up to ∞ can be seen. The transitions to $n=5$ or higher are not resolved and may cause an apparent edge shift to energies lower than those calculated. The energy values of the transitions for Si^{4+} ions can be found in literature.[15] The other transition energies, for Si^0 to Si^{3+}, can be approximated by Slater–Zener orbital calculations. For results see Table III. To get an impression of the accuracy of this method we also calculated the transition energies for Si^{4+} ions. In the calculation there is no difference between an s or a p electron. Therefore, we find an energy value between the actual position of these two possible transitions.

An important point that should be made in connection with the comparison with the earlier foil measurements is that the latter represents the absorption of both the foil and the particles emitted from the foil.

A. Energy density 3.5 J/cm^2

In Fig. 2(a) we see that the spectra are almost identical to those in Fig. 2(b). The edge, indicated by l-Si (liquid Si),

TABLE I. Position of the Si spectral features and their physical origin in the range between 90 and 190 eV.

	Symbol	Observed energy (eV)	Assignment	Expected energy (eV) (see Table III)
Edges	*l*-Si	105	liquid Si-$L_{II,III}$ edge	105[a]
	cl-Si	110	small clusters	...[b]
	Si^0	115	Si^0-$L_{II,III}$ edge	115.8[c]
	Si^{1+}		Si^{1+}-$L_{II,III}$ edge	125.4[c]
	Si^{2+}		Si^{2+}-$L_{II,III}$ edge	137.1[c]
	Si-L_I	150	Si-L_I edge	150[a]
	Si^{3+}		Si^{3+}-$L_{II,III}$ edge	152.0[c]
	Si^{4+}		Si^{4+}-$L_{II,III}$ edge	168.4[c]
Absorption peaks	*A*	95	Si^0 structure	?
	B	104	$2s^2\,2p^6$–$2s^2\,2p^5\,3s$ (Si^{4+})	104.7[d]
	C	127	$2s^2\,2p^6$–$2s^2\,2p^5\,3d$ (Si^{4+})	128.0[d]
	D	136	$2s^2\,2p^6$–$2s^2\,2p^5\,4s$ (Si^{4+})	136.8[d]
	E	145	$2s^2\,2p^6$–$2s^2\,2p^5\,4d$ (Si^{4+})	145.3[d]

[a] Values as observed in the foil measurements. See Ref. 8.
[b] Between *l*-Si and Si^0.
[c] See Ref. 14 (calculated by Hartree–Fock potentials).
[d] See Ref. 15.

can be seen in both spectra. From the foil measurements it was concluded that this is the $L_{II,III}$ edge of (short lived) liquid Si. This means that in Fig. 2(a) we are dealing with the L edge of Si in a state of aggregation having the same absorption characteristics as liquid Si. We believe that this is the $L_{II,III}$ edge of large sized Si clusters, or droplets. These clusters might be produced by the thermal strain of a superheated subsurface layer.[10]

B. Energy density 14.0 J/cm²

In Figs. 3(a) and 3(b) the absorption of what most likely is a cloud of ionized Si particles can be seen. In Fig. 3(a) there are peaks between 120 and 160 eV (peaks *C*, *D*, and *E*) and at 104 eV (peak *B*). These peaks are the same as those in Fig. 3(c) and can be assigned as absorption peaks of Si^{4+} ions (see Table I). Other clear structures in Fig. 3(a) are the Si^0, Si^{2+}, and Si^{3+} $L_{II,III}$ edges at approximately 115, 135, and 150 eV, respectively. The exact edge position is hard to determine because of the presence of unresolved Rydberg peaks at the low-energy side of the absorption edge, which can shift the apparent edges to lower energies than those calculated (see Table III). After 60 ns the edges of Si^{2+} and Si^{3+} disappear. Then only the $L_{II,III}$ edges of Si^0 and Si^{1+} can be seen, indicating recombination of the more highly charged species. This assignment is supported by the calculations in Table III. Peak *A*, at approximately 95 eV, is probably a Si^0 absorption line, because it is only present when the Si^0 edge is large. Due to the large uncertainty in the energy values in Table III it is not possible to assign peak *A*. The *L* edge for liquid Si is at approximately 105 eV,[8] and the *L* edge for large sized Si clusters is expected to be at the same position, while the *L* edge for Si^0 atoms is at 115 eV. Small sized clusters could be expected to have their edge somewhere in between, so we tentatively assign the edge at 110 eV, indicated by *cl*-Si, as the $L_{II,III}$ edge of small sized Si clusters, and the peak above the edge as an absorption peak of these clusters.

TABLE II. Summary of absorption features in Figs. 2–4.

	Particle emission from bulk Si					Foil transmission	
Energy density (J/cm^2)	3.5	6.0	6.0	14.0	14.0	0.7	3.6
Delay time (ns)	12	12	60	12	60	12	12
l-Si	S	S	S	...	...	S	S
Si^0	W	S	...	S	S	W	S
Si^{1+}	W	S	...	...	S	...	...
Si^{2+}	...	W	...	S	S	...	...
Si^{3+}	...	...	...	S	...	...	...
Si-L_I	...	...	S	...	...	S	S
cl-Si	W	S	S	W	S	...	...
A	...	S	...	S	S	...	S
B	...	...	...	S	...	...	...
C	W	W	...	S	W	...	S
D	...	W	...	S	W	...	S
E	...	...	...	S	...	...	S

(...)—absent.
W—weak.
S—Strong.

TABLE III. Energy values for transitions from $2s^2\,2p^6$ to $2s^2\,2p^5nl$, as determined by Slater–Zener orbital calculations, and $L_{II,III}$ edge positions for different ionization levels of Si.

	Slater–Zener orbital energy (eV)				$L_{II,III}$ edge energy (eV) from Hartree–Fock potentials[14]
	$n=3$	$n=4$	$n=5$	$n=\infty$	$n=\infty$
Si^0	103.6	113.7	115.3	115.9	115.8
Si^{1+}	103.5	119.8	122.2	124.9	125.4
Si^{2+}	104.2	126.5	130.9	135.8	137.1
Si^{3+}	92.5	134.3	146.8	148.4	152.0
Si^{4+}	107.5	141.7	149.3	162.9	168.4
Si^{4+}	104.7	136.8	153.1	See Ref. 15	
	128.0	145.3			

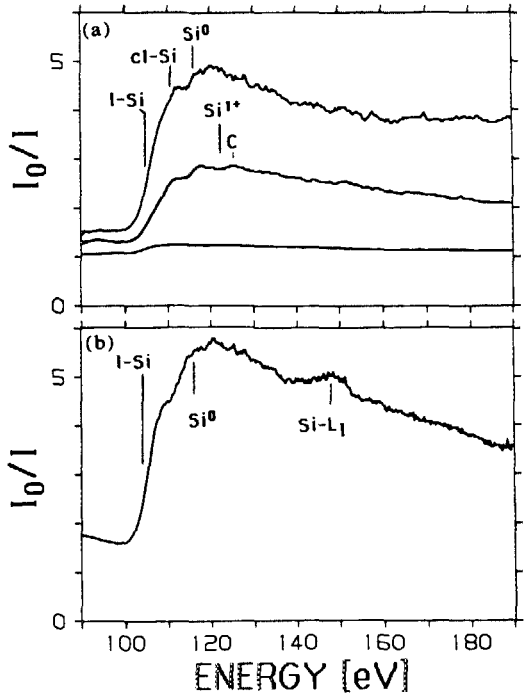

FIG. 2. (a) X-ray absorption spectra at a delay time of 12 ns between pump and probe beam and a pump beam energy density of 3.5 J/cm^2. The different spectra are recorded at different distances between emitting surface and probe beam. The distances are, from top to bottom, 100, 200, and 300 μm. (b) X-ray absorption spectrum from the earlier foil measurements,[8] recorded at a delay time of 12 ns and an energy density of 0.7 J/cm^2.

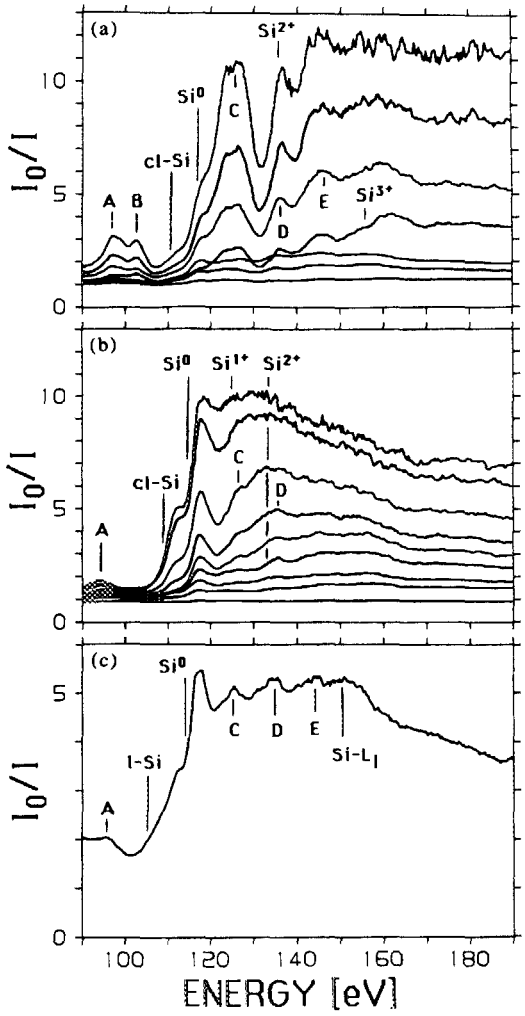

FIG. 3. (a) X-ray absorption spectra at a delay time of 12 ns between pump and probe beam and a pump beam energy density of 14.0 J/cm^2. The distances are, from top to bottom, 100, 200, 300, 400, 500, 600, and 800 μm. (b) Same as (a), except for the delay time and the distances. The delay time is 60 ns, and the distances are, from top to bottom, 100, 200, 400, 600, 1000, 1200, 1500, 2000, and 3000 μm. (c) X-ray absorption spectrum from the earlier foil measurements,[8] recorded at a delay time of 12 ns and an energy density of 3.6 J/cm^2.

In 60 ns the line structures become less pronounced, apparently clustering takes place, producing small sized clusters. According to Refs. 7 and 9, the size is something like 5 to 10 atoms per cluster.

C. Energy density 6.0 J/cm²

At this intermediate energy density there is, in Fig. 4(a), an indication of additional structure between 105 and 110 eV, which we assign as the edge for small sized clusters. Thus, in this case both the edges for small and large sized clusters are present. Also the Si^0 edge is present. Above this edge peaks *C* and *D* can be seen. These peaks are now assigned as edge structures due to Si^{1+} ions, because of the relatively low-energy density (see Table III). After 60 ns, the Si^0 edge decreases, see Fig. 4(b), while the *cl*-Si edge increases. This means that the atoms are combining to form small sized clusters. Figure 4(b) shows the only spectra with a clearly visible L_I edge. We do not have an explanation for the absence of the L_I edge in the other spectra.

D. General

There are in principle two distinguishable energy density regions in the particle production. This is a subdivision of range III, the damage range, for the foil measurements. In the low-energy density region, the surface layer and the subsurface layer melt. In this region liquid clusters (droplets) are emitted from the surface due to the thermal strain of the superheated subsurface layer.[10] In the high-energy density region a plasma is formed, which emits electrons and subsequently ions by the repulsive Coulomb force. At the boundary of these two regions the process of evaporation occurs, and neutral atoms are emitted from the surface.

In summary, the following picture emerges: at 3.5 J/cm^2 most emitted particles are large sized clusters (droplets) and neutral Si atoms. At 6.0 J/cm^2 there are small clusters, Si atoms, and Si^{1+} ions. At 14 J/cm^2 we find ionization states up to Si^{4+}. To obtain Si^{5+} ions, we should need an even higher energy density. The electron temperature in the plasma created at 14 J/cm^2 is approximately 50 eV.[16] This is lower than the $\approx$168 eV needed to ionize Si^{4+}.

For the foil damage range we found an onset at $\approx$1.0 J/cm^2, i.e., appearance of the Si^0 $L_{II,III}$ edge, while this is $\approx$3.0 J/cm^2 for bulk Si. The difference is due to the fact that the bulk of the Si acts as heat sink. In the case of a foil, the heat can only be transported lateral to the surface, for which more time is needed than for the bulk case, where the heat can dissipate perpendicular to the surface.

In all measurements performed as a function of the dis-

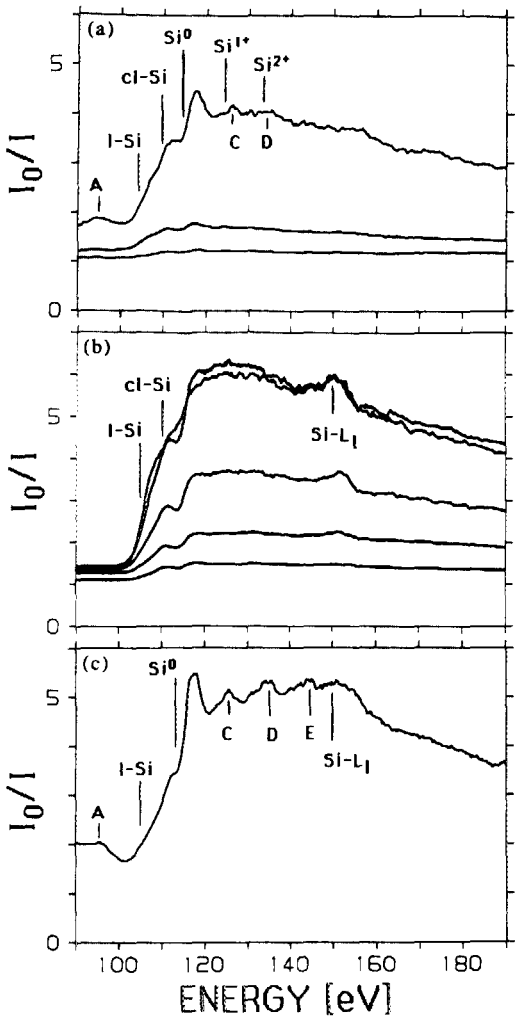

FIG. 4. (a) X-ray absorption spectra at a delay time of 12 ns between pump and probe beam and an energy density of 6.0 J/cm^2. The distances used are, from top to bottom, 100, 300, and 400 μm. (b) Same as (a), except for the delay time and the distances. The delay time is 60 ns, and the distances are, from top to bottom, 100, 200, 400, 800, and 1000 μm. (c) The same as Fig. 3(c).

tance to the emitting surface, it is found that the spectrum height and therefore the particle density decreases with increasing distance. For high-energy densities the decrease of the spectra is less than at low-energy densities. This indicates an increase of the particle velocity upon increasing the energy density. The maximum velocities of Si particles range from 2.5 to 5.0$\times 10^4$ m/s, depending on the energy density used. This was determined by simply taking the largest distance where absorption was measured, and dividing this value by the delay time. On increasing the distance to the surface, we found that the more highly charged ions have higher kinetic energies than the ions with lower charge. This can be seen very clearly for the measurements at 14 J/cm^2 after a delay time of 60 ns; the Si^0 edge height decreases, relative to the other structures, with distance. This is in good agreement with the model that the force emitting the ions from the surface is a repulsive Coulomb force. This force is produced by first emitting electrons, which creates a fast space-charge wave, and accelerates the ions.

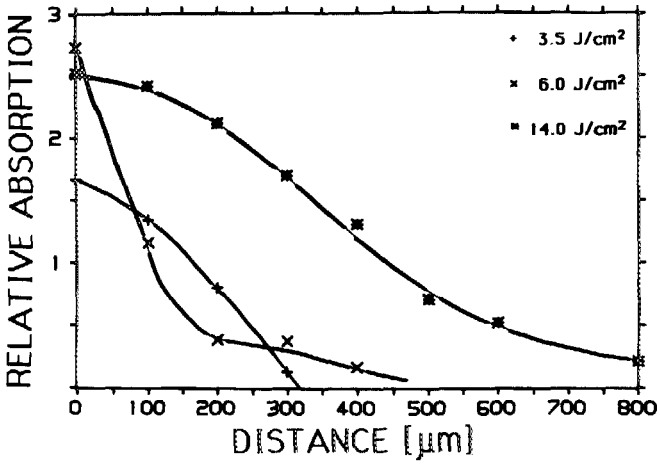

FIG. 5. Relative absorption by emitted-particle clouds as function of the distance above the surface, obtained from integral of $\mu(E)d$ in the 170–180 eV energy range for three different pump beam energy densities.

To determine the emitted layer thickness, we compared the absolute heights of the spectra described above with the measurement performed earlier on a 600-Å foil. For the foil measurement the number of absorbing atoms is known. Taking the logarithm of the I_0/I spectra one obtains $\mu(E)d$, i.e., absorption coefficient times thickness. We determined the integral of $\mu(E)d$ over the range 170–180 eV. We took this range, which is well above all the $L_{\text{II,III}}$ edges, since the $\mu(E)$ values of the different states of ionization and clustering are certainly not the same in the vicinity of edges. We make the assumption that the $\mu(E)$ values are the same in this energy range. Figure 5 shows the results for each $\mu(E)$ at various heights above the surface.

The numbers obtained by integrating over all heights are compared with the number from the Si foil measurement. From the ratio between these numbers we calculated the emitted layer thickness as a function of the irradiating energy density. The result is shown in Fig. 6, in which we see a steep threshold, followed by a plateau and then a nonlinear increase of the emitted layer thickness as function of the irradiating energy density.

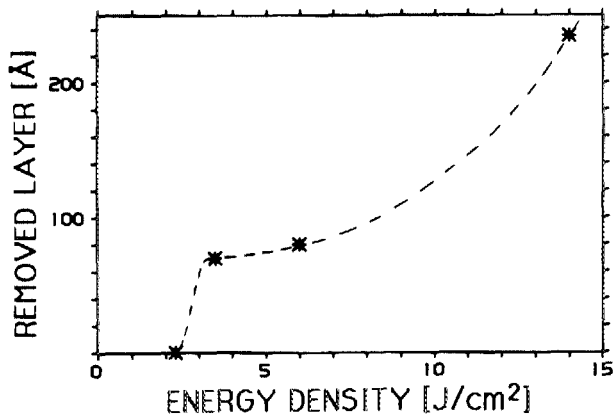

FIG. 6. Emitted Si layer thickness as function of the irradiance for 15 ns laser pulses of 532 nm light.

V. CONCLUSIONS

From the particle cloud absorption results we conclude that there are two energy density regions for the particle emission process from bulk Si. At low-energy densities (3–6 J/cm^2) large sized clusters, or droplets, are emitted. In the high-energy density region ($>6\ J/cm^2$) ions are emitted by a repulsive Coulomb force. The level of ionization increases with increasing energy density.

Clusters can be produced in both ranges. In the low-energy range large sized liquid clusters are formed. They exhibit the same edge shape as found for liquid Si foils. In the high-energy range, the process of recombination of ions and electrons is followed by clustering of the atoms into small sized clusters. This recombination process takes place on a timescale of several tens of nanoseconds.

The edge and the peak structure at 115 eV are believed to be absorption structures of the $L_{\mathrm{II,III}}$ edge of neutral Si atoms. This would be the first observation of x-ray absorption of atomic Si.

The removed Si layer thickness as a function of the energy density was determined; a typical number is ≈ 80 Å at ≈ 6 J/cm^2 at a pulse duration of 15 ns.

Si particle velocities range from 2.5 to 5.0×10^4 m/s. It was found that the highly charged ions move faster than the ions with a low charge number.

ACKNOWLEDGMENTS

The authors wish to thank Rob Kemper for technical assistance. This work is part of the research program of the Stichting voor Fundamenteel Onderzoek der Materie (Foundation for Research on Matter) and was made possible by financial support from the Nederlandse Organisatie voor Zuiver–Wetenschappelijk Onderzoek (Netherlands Organization for the Advancement of Pure Research).

[1] B. C. Larson, C. W. White, T. S. Noggle, J. F. Barhorst, and D. M. Mills, Appl. Phys. Lett. **42**, 282 (1983).
[2] K. Murakami and K. Masuda, in *Semiconductors Probed by Ultrafast Laser Spectroscopy*, edited by R. R. Alfano (Academic, New York, 1984), Vol. II, pp. 171–195.
[3] Kouichi Murakami, Hans C. Gerritsen, Hedser van Brug, Fred Bijkerk, Frans W. Saris, and Marnix J. van der Wiel, Phys. Rev. Lett. **56**, 655 (1986).
[4] J. M. Lui, R. Yen, H. Kurz, and N. Bloembergen, Appl. Phys. Lett. **39**, 755 (1981).
[5] L. A. Bloomfield, R. R. Freeman, and W. L. Brown, Phys. Rev. Lett. **54**, 2246 (1985).
[6] D. Lubben, S. A. Barnett, K. Suzuki, S. Gorbatkin, and J. E. Green, J. Vac. Sci. Technol. B **3**, 968 (1985).
[7] L. A. Bloomfield, M. E. Geusic, R. R. Freeman, and W. L. Brown, Chem. Phys. Lett. **121**, 33 (1985).
[8] H. C. Gerritsen, H. van Brug, F. Bijkerk, K. Murakami, and M. J. van der Wiel, J. Appl. Phys. **60**, 1774 (1986).
[9] D. Tomanek and M. A. Schlüter, Phys. Rev. Lett. **56**, 10 (1986).
[10] J. F. Ready, *Effects of High Power Laser Radiation* (Academic, New York, 1971).
[11] H. C. Gerritsen, H. van Brug, M. Beerlage, and M. J. van der Wiel, Nucl. Instrum. Methods **238**, 546 (1985).
[12] H. C. Gerritsen, H. van Brug, F. Bijkerk, and M. J. van der Wiel, J. Phys. E (in press).
[13] H. C. Gerritsen, H. van Brug, F. Bijkerk, and M. J. van der Wiel, J. Appl. Phys. **59**, 2337 (1986).
[14] Enrico Clementi, Tables of Atomic Functions, San Jose Research Lab., IBM Corp., San Jose, California.
[15] R. L. Kelly and L. J. Palumbo, NRL Report 7599, June 1973.
[16] D. W. Forslund, J. M. Kindel, and K. Lee, Phys. Rev. Lett. **39**, 284 (1977).